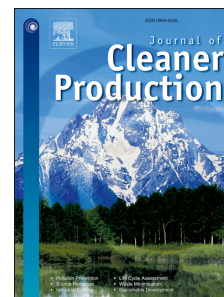# Accepted Manuscript

Integrated energy analysis of cutting process and spindle subsystem in a turning machine

Jeremi Wójcicki, Marco Leonesio, Giacomo Bianchi

Please cite this article as: Wójcicki J, Leonesio M, Bianchi G, Integrated energy analysis of cutting process and spindle subsystem in a turning machine, *Journal of Cleaner Production* (2017), doi: 10.1016/j.jclepro.2017.09.234.

Integrated energy analysis of cutting process and spindle subsystem in a turning machine

Jeremi Wójcicki*, Marco Leonesio, Giacomo Bianchi

Istituto di Tecnologie Industriali e Automazione, Via Alfonso Corti 12, 20133, Milano, Italy

*Corresponding author. E-mail: jeremi.wojcicki@itia.cnr.it

Abstract

This paper presents a novel approach for systematic energy efficiency evaluation and optimization in turning operations, combining spindle, chiller and material removal models. Framing a joint machine-process design approach, the proposed study aims at selecting optimal combinations of cutting parameters (feed rate, depth of cut and spindle speed) for a given spindle-chiller assembly, able to minimize the energy consumption. Contrary to most of the literature, where the efficiency analysis is fully empirical, relying on extended cutting test campaigns, here a model-based approach is adopted. The goal is to characterize a key subsystem of modern machine tools, often used in both turning and milling machines, composed by a permanent magnet brushless direct-drive spindle with a dedicated chiller unit. Analytical relationships are identified, producing efficiency maps as a function of various process parameters. Physic-based models are exploited, reproducing electrical and mechanical energy dissipation occurring in the spindle and chiller units and in the material removal process. The models parameters are identified by a reduced set of spindle ramp-up and cutting tests, executed in an industrial context. Then, an overall process efficiency optimization is performed and discussed.

Keywords: Turning, process efficiency, energy models, spindle, chiller

1. Introduction

Correct selection of cutting parameters in machining is very important to achieve the prescribed quality with an economical, productive process. The choice is driven by various criteria, to assure the required accuracy of the workpiece and surface integrity, with an optimal balance between production rate and production cost. A multi-objective optimization

of process planning can tackle vibration and tool life issues (Leonesio et al., 2012); similarly, productivity and chatter avoidance criteria can be used to control spindle speed and feed rate for a generic milling process (Bort et al., 2016). Statistical methods were employed for best parameter selection in turning, aiming at surface roughness and tool life improvements (Yang and Tarng, 1998).

In recent years, a wide attention has been devoted to machine tools (MTs) environmental impact, which is usually dominated by energy consumption in the use phase. A pioneering attempt to outline a systematic approach for including energy efficiency objectives in manufacturing systems and processes is provided by Duflou (2012), while a recent and comprehensive review can be found in Zhou (2016). MTs efficiency in terms of overall energy consumption with respect to productivity has been analyzed experimentally by Diaz et al. (2010, 2011) outlining the importance of machining time in energy demand prediction. A multi-objective optimization model including energy demand together with other performance indicators, like costs, on heavy-duty CNC has been introduced by Xiong et al. (2016), to assist optimal process parameters selection. In this work, spindle rated power and utilization factor parameter were used to represent a spindle energy model. Simulation based tools and methodologies were investigated to predict MT energy consumption during generic work piece machining (Borgia et al., 2016). One major issue concerns the link between specific consumed energy in machining, i.e. the ratio between energy spent per volume of material removed, and the parameters that could have an influence on it. In fact, these parameters modify both the power used by the MT, where in this sense the main spindle is usually responsible for the majority of the expenditure, and the amount of material removed (Borgia et al., 2014b). Albertelli et al. (2016) proposed a model to estimate energy demand of production cycle in a milling machine including influence of MT peripheral subsystems, however using assumption of constant spindle efficiency, whereas Peng and Xu (2013) introduced a hybrid model for a CNC machine, which utilized experimental model of both process and spindle energy demand. An experimental study on the influence of main

cutting parameters (feed rate, axial depth of cut, radial depth of cut, cutting speed) on both MT efficiency and specific energy consumption for turning machines was conducted by Draganescu (2003). A similar analysis was performed later by Mori et al. (2011), examining the effects of cutting parameters on total energy consumption in face-milling operations. Both works state that, during machining, the most relevant energy usage is due to the spindle unit, which performs the material removal.

Following the track outlined by Draganescu (2003), the present article tackles the problem of optimal cutting strategy in turning operation by performing an integrated analysis of the efficiency of the core subsystem of a MT: the spindle-chiller assembly, herein denoted as Processing Unit (PU). On the contrary to several studies presented above, where either purely experimental models or cutting process analytical models with simplified representation for spindle subsystem (e.g. with motor constant efficiency) are used, authors employ a holistic, physical model, integrating cutting process, spindle assembly, spindle motor and chiller unit sub-models. The joint machine - process analysis approach supports the selection of the optimal combination of cutting parameters (feed rate, depth of cut and spindle speed) for a given PU, able to minimize the energy consumption during machining. Additionally, the analysis provides useful data to machine designers, about losses and efficiency of spindle and chiller during reference machining operations. Coherently with the industrial practice, spindle and chiller are considered as a coupled elementary unit: in a "what if" analysis comparing different possible PU combinations, e.g. based on induction or synchronous motors, an efficiency comparison must consider also the different requirements in terms of motor cooling.

On the contrary to works of Draganescu (2003) and Mori et al. (2011), where the efficiency analysis is fully empirical, relying on extended cutting test campaigns, in this article a model-based approach is adopted and validated by experiments. Analytical relationships are identified, providing efficiency maps as a function of the various process parameters. The models are based on the systems physics, taking into account electrical and mechanical

energy dissipation, which occurs both in PU and in the material removal process. The models parameters identification can be carried out exploiting a reduced set of experiments (spindle ramp-up and cutting tests); then, once validated, models can be used to get a general insight about process efficiency.

This paper proposes, for a given work piece (described by its diameter d) and MT, to optimize process parameters to minimize the used energy E, for each possible level of Material Removal Rate (MRR). The obtained relationship, $E = f(d, MRR)$, contains the dominant solutions and constitutes a Pareto front for possible subsequent global optimizations. Even though this work is focused on PU efficiency, a global MT energy optimization is guaranteed because the MRR is related to the machining time. It is therefore possible to evaluate the overall cutting specific energy (Diaz et al., 2010) taking into account the contribution of the basal consumption of other MT peripherals (e.g. the process coolant pump), that can be considered as independent from the activity of PU and only proportional to the overall processing time. A sample application, explored in this article, is the reduction of specific energy obtained decreasing the *MRR*, as suggested by Avram and Xirouchakis (2011).

The paper is structured as follows. Section 2 states the problem and scope of the study. In section 3, the energy models of spindle, chiller and material removal processes are presented. Section 4 is devoted to model parameters identification: the measurement setup used to feed the identification system is described; then, parameters are identified via Least Squares method and validation is performed according to a *k*-fold approach. Section 5 presents the main result of the study: the energy optimization of a cylindrical turning process (in terms of feed rate, spindle speed and depth of cut). This goal is achieved through computation of the integrated efficiency map of the PU and material removal process. Discussion and conclusions are reported in section 6 and 0, respectively.

2. **Problem statement**

PU efficiency depends on its thermo-electromechanical characteristics and on spindle velocity and torque, required to machine the work piece material with given process parameters. Thus, an effective PU energy optimization must include the cutting process. The objective of the present article is establishing, for given PU, workpiece material, tool and *MRR*, the optimal cutting parameters that minimize the process energy consumption. The goal is achieved by coupling a mechanistic model of material removal with the thermo-electro-mechanical model of the PU. Since the efficiency is expressed as a function of *MRR*, the resulting relationship can be exploited to carry out the overall machining energy optimization at MT level, once all the other energy consumers in the machine are known. In formula, for a turning process and parametrizing the result with respect to bar diameter, the problem can be stated as follows:

$$\eta_{max}(MRR|d) = \begin{cases} \max\limits_{a_p, f, \omega} \ \eta(a_p, f, \omega, d) \\ s.t. \ a_p \cdot f \cdot \omega \cdot \dfrac{d}{2} = MRR \end{cases} \tag{1}$$

Following the proposed approach, a PU unit of a CNC lathe is identified and analyzed. The obtained results allow, on one side, to optimize the cutting parameters and, on the other side, to asses a PU design for a given set of reference operations. The proposed approach can be applied to all spindle equipped with brushless motors, that are more and more common: to obtain quantitative results, the identification and analysis procedures must be executed on spindle-chiller assembly of interest.

3. Energy models of the processing unit and the material removal process

3.1. Energy model architecture

System under consideration is a PU (a spindle-brushless motor-chiller assembly), which performs a material removal operation (Fig. 1). In this section state of the art models of electric motor, spindle and chiller losses are used to assemble a complete model of the PU. PU efficiency η_{PU} is the ratio of useful mechanical output, used for cutting, and electrical power demand of both spindle and chiller. Whereas spindle efficiency is a function of cutting

torque and speed, chiller demand depends on its basal power and heat load delivered by the spindle, because of its internal resistive and friction losses.
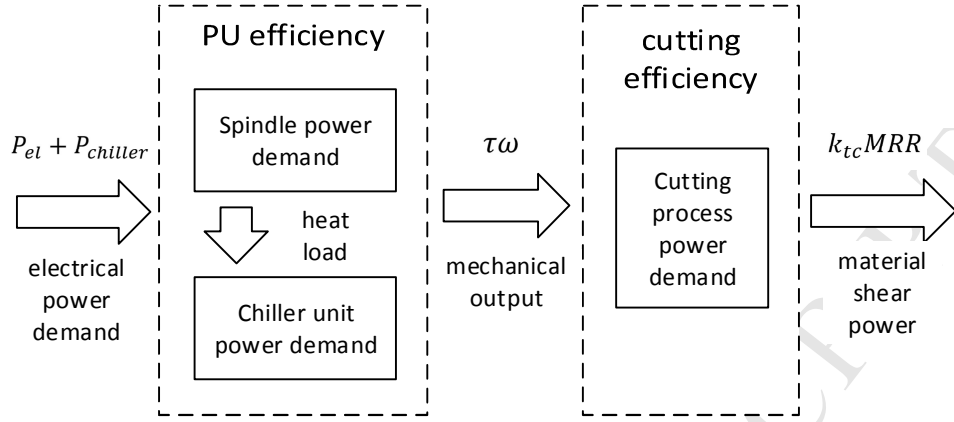

Fig. 1. Architecture of efficiency models of PU and cutting process.

Cutting process efficiency η_{cut} is expressed as ratio of material shear power and mechanical input power used in that process. For a given tool, shear power corresponds to the product of the material specific energy (k_{tc}) and the adopted *MRR* and is theoretically the minimum value of energy needed to remove a certain volume of material. Overall efficiency is therefore a product of cutting process efficiency and processing unit efficiency, which incorporates both spindle and chiller subsystems:

$$\eta(a_p, f, \omega, d) = \eta_{PU} \cdot \eta_{cut} \qquad (2)$$

3.2. Spindle energy model

The examined turning machine was equipped with a direct drive spindle with a permanent magnet synchronous motor. Energy demand of spindle is a function of two inputs – spindle speed and external load torque:

$$P_{el} = f(\tau, \omega) = K_T i_q(\tau)\omega + P_{mot\ loss} \qquad (3)$$

Electrical power demand consists of two components – effective, mechanical output power and electrical power losses. The latter is represented usually as iron and copper losses, related to heat generated respectively in the magnetic core and in the copper windings. In this article, only copper loss component will be considered (following the approach

presented in (Albertelli et al., 2011) and extending the model derived in (Wójcicki et al., 2016)):

$$P_{mot\ loss} = 3R(i_q^2 + i_d^2) \tag{4}$$

Direct and quadrature currents are set by the adopted control strategy, where the quadrature current i_q is a function of the required torque and the direct current is used to generate defluxing, when a threshold velocity is exceeded:

$$i_q = \frac{\tau_{load}(\tau)}{K_T} \tag{5}$$

$$i_d = \max\left(0, \alpha\left(\frac{1}{\omega_0} - \frac{1}{\omega}\right)\right) + \beta|i_q| \tag{6}$$

Rotor dynamic equilibrium relates static and viscous friction, rotor and spindle inertia and motor output ("load") torque:

$$\tau_{load}(\tau_{cutt}, \omega) = sign(\omega)\mu_s + \omega\mu_v + J\dot{\omega} + \tau_{cutt} \tag{7}$$

3.3. Chiller energy model

The chiller is composed by the refrigeration circuit, the pump that recirculates the coolant fluid and the electronic equipment. Considering the classic case of a constant speed pump, its power consumption, as for the electronic system, is constant. The compressor average power consumption is assumed to be proportional to the total heat load. The resulting energy model is then given by a linear relationship, as in (Borgia et al., 2014a):

$$P_{chiller} = P_b + \frac{P_h(\omega, \tau)}{\theta} \tag{8}$$

Base power consumption P_b includes the power demand of the chiller pump and the part of the compressor power that is used to remove the heat injected by the chiller pump into the cooling circuit. The θ coefficient determines the effectiveness of the cooling. It will be assumed that all the non-productive output power of the spindle, namely friction and copper

losses, is turned into heat load for the chiller (i.e. neglecting, at steady state, heat transfer to the machine body and the environment):

$$P_h(\omega, \tau) = (\tau_{load}(\tau_{cutt}, \omega) - \tau)\omega + P_{mot\ loss}(\tau_{load}, \omega) \tag{9}$$

The considered turning machine tool is equipped with a chiller that is dedicated to spindle thermal control. Parameters of the chiller model are given in Table 1.

Table 1. Chiller model parameters

Parameter name	Parameter value
P_b	1780 [W]
θ	4.64 [-]

3.4. Efficiency of spindle and chiller assembly

Spindle efficiency is a ratio of the useful mechanical output power to the electrical power demand. Torque loading due to spindle inertia is only significant in the model identification phase, to properly characterize effective output power. Typically, during material removal, spindle speed is constant, therefore for efficiency analysis of the cutting process the inertial torque term $J\dot{\omega}$ can be omitted.

$$\eta_{spindle}(\tau, \omega) = \frac{\tau\omega + J\dot{\omega}}{P_{el}(\tau, \omega)} \xrightarrow{\dot{\omega} \equiv 0} \frac{\tau\omega}{P_{el}(\tau, \omega)} \tag{10}$$

Spindle motors require appropriately scaled cooling systems. For direct drive electro-spindles, an external chiller is a common solution, whereas in case of mechanical spindles with external motor, often air cooling is sufficient. Because these two subsystems are tightly bonded together, a machine designer that considers efficiency of different spindle alternatives should include energy demand of cooling system in the overall efficiency calculation. For that reason, we extend the definition of spindle efficiency to include cooling system as well, as formalized in Eq. (11). As the cooling system does not provide usable output for removal process, it will only affect the denominator of the efficiency function:

$$\eta_{PU}(\tau, \omega) = \frac{\tau\omega}{P_{el}(\tau, \omega) + P_{chiller}(\tau, \omega)} \tag{11}$$

Such a formulation allows direct comparison of efficiency between several types of spindle systems, which seem to be more practical for day-to-day choices in energy aware design and configuration.

3.5. Cutting process model

The mechanical specific energy is also known as "cutting coefficient" and it is the key parameter for computing cutting power and torque: it depends on the tool and the work piece material properties and it is often provided by tool suppliers to verify machine cutting capability constraints during process planning. Let a longitudinal turning operation be considered, where a_p denotes the depth of cut, f the feed per turn, v_c the cutting speed, ω the spindle speed and d the average cut diameter. The *MRR* expression becomes:

$$MRR = a_p f v_c = a_p f \frac{d}{2} |\omega| \tag{12}$$

Then, the mechanical specific energy k_c can be expressed as the ratio between cutting power and *MRR*, the former being equal the tangential cutting force component multiplied by the cutting velocity. Namely:

$$k_c = \frac{P_c}{MRR} = \frac{F_c v_c}{MRR} = \frac{F_c \omega d}{2MRR} \tag{13}$$

A great amount of past scientific works dealt with cutting force modelling (e.g. (Ehmann et al., 1997) and (Arrazola et al., 2013)) and with turning process in particular (e.g., (Dong et al., 2009)). All of them consider both the force originated by material shear (cutting component, proportional to chip section) and friction in the contact area between the tool flank face and the workpiece surface (edge force component, proportional to the depth of cut). In the simple and very widespread model proposed in (Altintas, 2012), the tangential cutting force component assumes the following expression:

$$F_c = (k_{te} a_p + k_{tc} a_p f) \tag{14}$$

The process coefficients appearing in Eq. (13) depend on tool properties (characteristic angles, coating, etc.), workpiece material and lubrication condition, thus, they must be

identified and/or estimated for each tool-workpiece combination. Moreover, cutting force is often influenced by cutting velocity, which is herein neglected. More comprehensive models would give a more accurate force prediction, but the corresponding increased complexity would not be compensated by significant enhancements in the results. By substituting Eq. (12) and Eq. (13) into Eq.(14), a formula for mechanical specific energy can be obtained. This expression suggests, to reduce the energy use, increasing as much as possible the feed per turn:

$$k_c = \left(\frac{k_{te}}{f} + k_{tc} \right) \tag{15}$$

Efficiency of the cutting process can be written as a ratio of useful power spent on the effective material shear to the mechanical output power of the spindle:

$$\eta_{cut}(a_p, f, \omega) = \frac{k_{tc} MRR}{\omega \tau} \tag{16}$$

3.6. Overall energy efficiency

The overall energy consumption can be decomposed into the energy used by the spindle and the associated chiller unit (E_{PU}), the "basal" energy consumed by the machine peripherals (E_0) and the energy used by machine axes to counteract cutting forces and friction. The latter component is usually negligible in roughing (Calvanese et al., 2013). Then, the overall energy consumption can be approximated as follows:

$$E_c = E_{PU} + E_0 \tag{17}$$

Spindle and chiller energy demand depends on the mechanical energy required by the tool for material removal and on the efficiency of spindle and chiller themselves:

$$E_{mech} = \eta_{PU} E_{PU} \tag{18}$$

Differentiating overall energy consumption E_c with respect to time and dividing both by *MRR*, an overall specific energy for cutting process (including efficiency of both spindle and chiller) is derived:

$$e_c = \frac{k_c(f)}{\eta_{PU}(a_p, f, v_c, d)} + \frac{P_0}{MRR(a_p, f, v_c)} \tag{19}$$

It may intuitively seem that increasing *MRR* through modifying process parameters a_p, f, v_c can minimize energy consumption (the right term) by reducing the contribution of machine basal power. However, it is not that obvious, considering the variable PU efficiency, which is function of the same parameters. Also, specific cutting energy depends on the feed, and behavior of these two terms influences the optimal choice of *MRR*. Workpiece diameter d is not to be considered a decision variable, as it is upfront defined by workpiece size. However, in the energy analysis of PU we consider a range of possible diameters, as they do influence efficiency functions and therefore may change optimal values for cutting parameters and resulting *MRR*.

4. Identification of spindle and cutting process models

4.1. Measurement setup

The experimental campaign has been performed on a two-spindle, 5-axis numerically controlled lathe: DMG MORI SPRINT 65-3T. Tests were performed on the main spindle of the machine. The machine is equipped with an automatic loader for 65mm bars. Parts can also be loaded by hand or through a robotic arm, and then the maximum size depends on the used chuck (125mm diameter with standard chuck). As mentioned before, the lathe is equipped with PM direct-drive spindle with a dedicated chiller unit for motor temperature control.

In terms of data acquisition, speed and motor currents (namely, direct current i_d and quadrature current i_q) have been sampled at 1kHz by machine numeric control. Simultaneously, instantaneous power demand was measured by proprietary three phase fast sampling power meter with +/-1% precision. Voltage probes and DC current sensors LEM-HAS100 were placed at the input to spindle motor and chiller unit (Fig. 2). Current and

voltage signals were sampled, after anti-aliasing pre-filtering, at 20ksps/channel. Active

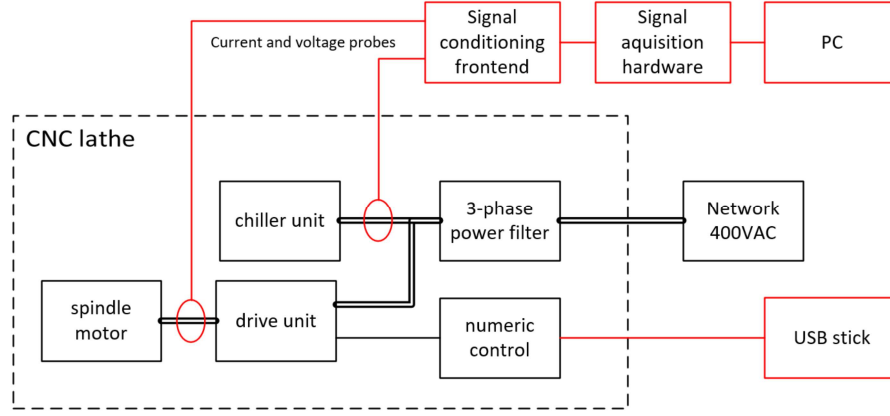power of each phase is computed at the frequency of 50Hz.

Fig. 2. Simplified schematic of the machine tool with indicated measurement points. Elements of acquisition system are marked in red.

In the performed tests, no external loading motor was used. To quantify mechanical output

of the spindle its moment of inertia has been utilized, imposing continuous acceleration and

deceleration, emulating therefore an external load.

4.2. Spindle three steps identification

Parameters identification of spindle energy model is performed by means of a cascade

approach. Each step analyses, separately, field weakening, power adsorption and overall

torque model:

1) α, ω_0, and β are identified from Eq. (5) knowing i_q, i_d and ω;

2) K_T and R are identified from Eq. (3) and Eq. (4) knowing i_q, i_d and P_{el};

3) μ_S, μ_v and J are identified from Eq. (7) knowing i_q and K_T.

Collected dataset consists of 1560 data samples of each quantity (i_q, $i_{d,}$ ω, P_{el}), thus the

same number of equations can be written for each step. As there are 3 unknowns in step *1)*

and 2 unknowns in steps *2)* and *3),* a least squares approach is used to solve the

overdetermined problem. Since the fact that the above-mentioned models are nonlinear the

solution is obtained numerically using the well-known *Levenberg-Marquardt* algorithm

(Marquardt, 1963). *MATLAB Optimization Toolbox* was employed to numerically perform

parameter identification as prescribed in (Geletu, 2007). The identified parameters are reported in Table 2.

Table 2. Estimated spindle model parameters

Parameter name	Identified value
α	8794 [A·rad/s]
ω_0	135 [rad/s]
β	0.404 [-]
K_T	5.4 [Nm/A]
R	0.223 [Ω]
μ_s	1.19 [Nm]
μ_v	0.042 [Nm·s/rad]
J	0.524 [kg·m^2]

The average relative residual errors on the three fittings are rather limited (see Table 3): the most significant one is related to torque model and it is lower than 10%. The soundness of the fitting can be appreciated, also graphically, in Fig. 3, Fig. 4 and Fig. 5, which are, respectively, the field weakening model fitting, the torque fitting over time and the power fitting over time.
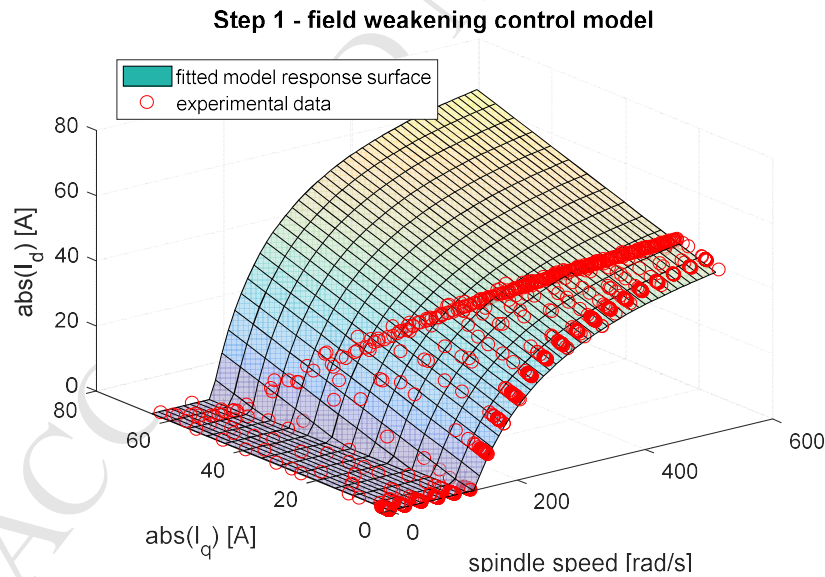

Fig. 3. Motor field control model fitting from Eq. (6), relating direct current component with spindle speed and quadrature current.
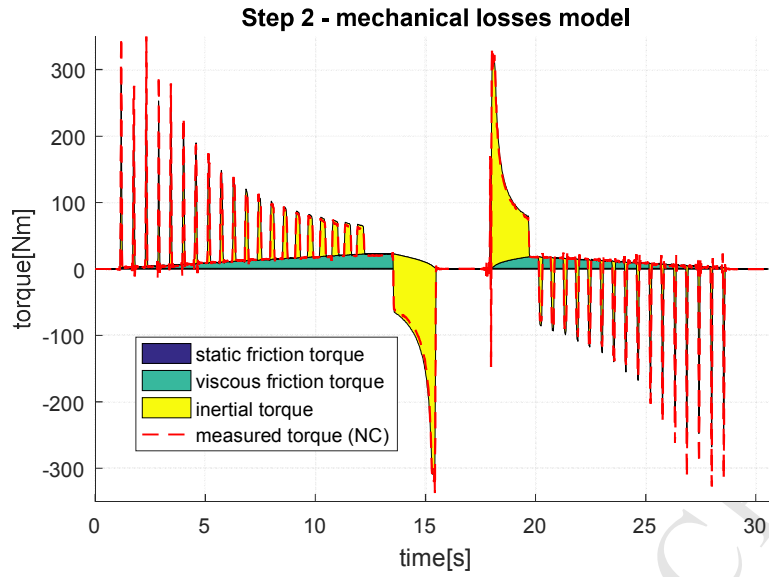
Step 2 - mechanical losses model

Fig. 4. Torque fitting over time

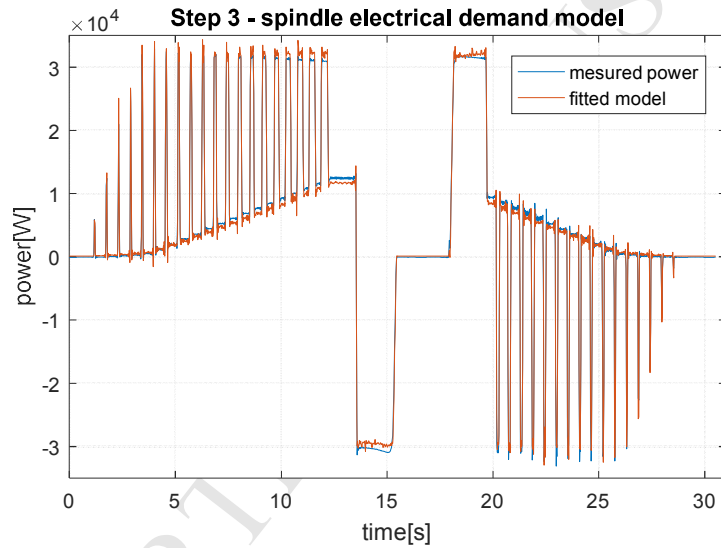**Step 3 - spindle electrical demand model**

Fig. 5. Electrical power fitting over time

Table 3. Relative fitting error in 3-step identification

Identification step	Relative fitting error
Step 1: field weakening model	2.08%
Step 2: power fitting model	6.09%
Step 3: torque model	9.83%

4.3. *K*-fold validation of the spindle model

The residual analysis is usually not enough to evaluate the predictive capability of fitted

models: prediction error estimation is also required to fully evaluate their efficacy. When

dealing with complex nonlinear models, like in the case of the spindle, cross-validation is

widely used to estimate the prediction error, that is usually better than residuals. The

problem with residual evaluations is that they do not give an indication on how well the

model will behave when it is asked to make new predictions for data that have not been used for parameters identification. Even though a leave-one out cross-validation is widely studied, *K*-fold cross-validation may be preferred from a computational standpoint (Stone, 1974). The data set is divided into *k* subsets, and the holdout method is repeated *k* times. Each time one of the *k* subsets is used as the test set and the other *k-1* subsets form the training set. Then, the average error across all *k* trials is computed.

After a randomization of the 1560 data samples, a *k*=10 cross-validation has been performed for spindle model identification. Parameters deviations across the 10 identifications are presented in Table 4. Relative deviations are very limited, except for static friction coefficient of the torque model (μ_s) that reaches 40%. This high error is due to the quite negligible contribution of static friction in determining the spindle torque, which makes this parameter almost unidentifiable.

Table 4. Parameters deviations (min., max. and average) across the *k*=10 folds

Parameter	α	ω_0	β	k_t	R	μ_s	μ_v	J
min.	0.00%	0.00%	0.06%	0.02%	0.04%	0.40%	0.01%	0.02%
avg.	0.12%	0.04%	0.70%	0.06%	1.38%	16.20%	1.15%	0.13%
max.	0.22%	0.10%	1.55%	0.21%	3.24%	36.37%	3.18%	0.26%

The mean relative fitting errors pertaining to the three models are depicted in Fig. 6. Even if the residuals have been computed on a data set that has not been used for the training, errors are rather limited and similar to those obtained for the whole data set (Table 3). Therefore, overfitting problems can be excluded.
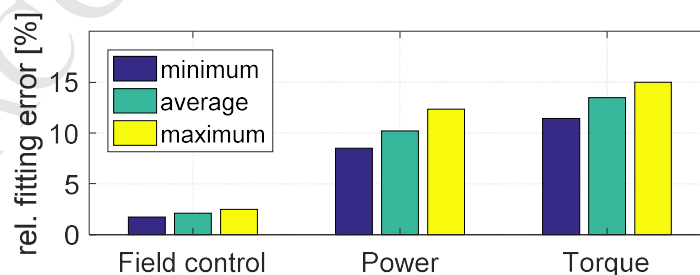

Fig. 6. Mean relative errors in the three steps of identification across the validation sets

4.4.   Cutting model identification

Cutting tests were performed with 8 combinations of feed and depth of cut (Table 5), using

DNMG 15-06-04-PM-4325 chip breaker by Sandvik Coromant™. Material was removed from

cylindrical test samples of 65mm in diameter, made of medium-carbon steel C45, and cutting

force model identified. Motor quadrature current was saved by the machine control system

as a proxy for torque measurement. Depending on the depth of cut, different number of tool

passes were performed, from 3 to 10, for a total of 42 passes. It has to be noted that the

proposed cutting tests are just aimed at identifying model parameters for the specific

combination of tool and workpiece material, while the validation of the model itself, together

with the limits in cutting parameters extension, can be found in (Altintas, 2012). Relying on

literature claims, in section 5 and 6 model predictions will be extrapolated to broader ranges

of feed per revolution and depth of cut.

Table 5. Performed cutting tests configuration

	Feed per revolution [mm]	Depth of cut [mm]	Chip cross-section area [mm^2]	Average torque [Nm]
1	0.20	4.0	0.800	40.10
2	0.30	3.0	0.900	43.86
3	0.20	3.0	0.600	30.43
4	0.30	2.0	0.600	35.25
5	0.15	2.5	0.375	23.95
6	0.25	1.5	0.375	21.72
7	0.10	2.0	0.200	13.93
8	0.20	1.0	0.200	11.07

Cutting torque was computed as a product of measured quadrature current and identified

motor torque constant. To fit the linear model of cutting forces from section 3.5, a least

square method was used. Estimated coefficients and fitting errors are presented in Table 6.

Adjusted coefficient of determination R^2 is 0.9687 and the condition number of the

observation matrix is 16.8. Based on the statistical analysis of the goodness of fitting, cutting

forces coefficients have been identified with high level of confidence and precision.

Table 6. Cutting parameter estimation and statistical goodness of fitting

parameter	estimate	squared error	t-statistic	p-value
k_{te} [N/mm]	63.82	20.39	3.13	0.00325
k_{tc} [N/mm^2]	1705.1	91.14	18.7	2.19e-21

4.5. Optimal cutting condition in function of *Material Removal Rate* and *workpiece diameter*

To explore most efficient strategies for material removal with the considered PU, the problem described by Eq. (1) has been set up: it maximizes the overall efficiency of PU and cutting process. Maximization procedure was repeated for a range of possible *MRR* and cutting diameters, which allows to explore energy performance under various production conditions. Varying diameter serves the purpose of representing different workpiece sizing and is important to understand how well the given PU is suited for a certain type of production mission. Varying *MRR* is used to explore possibility of reducing overall performance in terms of material removal for the sake of energy saving. Spindle continuous operating region (also known as S1 duty cycle (Drury, 2001)) has been imposed in form of a set of constraints limiting spindle mechanical output power, torque and speed:

$$\begin{cases} \omega \tau_{load}(a_p, f, \omega) \leq P_{max} \\ \tau_{load}(a_p, f, \omega) \leq \tau_{max} \\ \omega \leq \omega_{max} \end{cases} \tag{20}$$

Limits related to tool impose certain minimum and maximum values of cutting speed, feed rate and depth of cut, for the given workpiece material:

$$\begin{cases} v_{c\,min} < v_c(\omega) \leq v_{c\,max} \\ f_{min} \leq f \leq f_{max} \\ a_{p\,min} \leq a_p \leq a_{p\,max} \end{cases} \tag{21}$$

Each workpiece diameter defines a certain maximum *MRR* which can be achieved by PU (due to PU and tool constraints). These values are found by solving an optimization problem in Eq. (22) for every diameter of interest and will formulate a starting point for efficiency maximization.

$$MRR_{max}(d) = \max_{a_p, f, \omega} MRR\,(a_p, f, \omega|d) \tag{22}$$

To perform numerically a multidimensional constrained nonlinear minimization for problems formulated in Eq. (1) and Eq. (22), an *active-set* (Hazewinkel, 1988) method has been used.

This numerical method is capable of handling bounded parameters and multiple constraints presented above.

5. **Results**

5.1. Process Unit efficiency map

Based on the identified models of the spindle and chiller, efficiency maps of the spindle (Fig. 7a) and of the PU (Fig. 7b) have been computed, according to the Eq. (10) and Eq. (11). Range of speed and torque corresponds to spindle capabilities: maximum speed of 6000rpm and maximum torque of 350Nm. The maximum power line, which limits the operating region of the spindle, has been marked on both plots by a continuous line, as well as rotor field weakening start speed, by the dashed line.
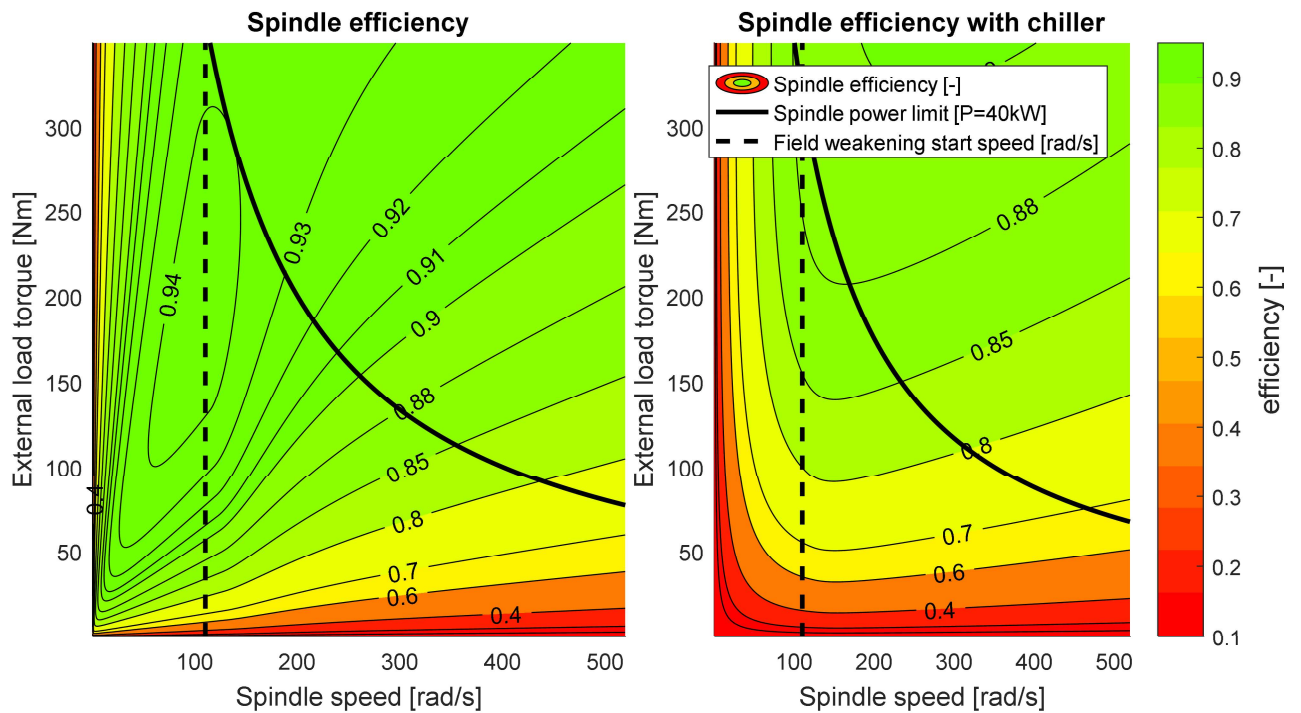

Fig. 7. a) efficiency map of the spindle; b) efficiency map of a spindle-chiller pair (PU)

Spindle alone reaches a maximum efficiency of around 94% at low speed (500-2000rpm) and optimal torque of around 200Nm at 1000rpm. Spindle is least efficient at high speed and low torque (typical of finishing operations), where efficiency can drop to 50% or below. This effect can be attributed to the high ratio between friction losses and useful output power.

Similarly, very low efficiency region occurs at high torque loading and very low speed, due to high resistive losses (proportional to τ^2) and little useful output power.

Introducing the chiller into overall PU efficiency assessment significantly reshapes the map. Maximum efficiency drops down to ~88% and occurs in a small portion of spindle operating region: high torque at speed close to field weakening starting speed (~1000rpm). Chiller contribution affects less high productivity regions – close to the spindle power limit, as its basal power consumption is relatively small with respect to spindle effective output power.

5.2. Efficiency of the cutting process with a spindle-chiller pair

Overall efficiency surfaces as a function of cutting parameters were drawn, based on the identified PU and cutting process model, from Eq. (2). Three values of cutting diameter were considered – small (20mm), medium (100mm) and large (300mm), corresponding to different sizes of workpieces that could be produced on the examined machine. To visualize efficiency for a wide range of parameter values, several working points were chosen to define 2D intersections in the 3D efficiency space (Table 7). Working points which are marked on the plots have been arbitrarily chosen for each considered cutting diameter to show representative features of the efficiency surfaces. Table 8 collects limits of the parameter that were used in efficiency surfaces generation. *Iso-MRR* lines were drawn to underline how moving along certain dimension may affect productivity of the material removal process.

Table 7. Arbitrary working points for 3D efficiency surfaces intersections

Diameter [mm]	Depth of cut [mm]	Feed [mm/rev]	Spindle speed [rpm]
20	5	0.2	2600
100	6	0.2	800
300	4	0.15	250

Table 8. Parameter ranges used in efficiency optimization corresponding to spindle/chip breaker limits

Parameter	Lower limit	Upper limit

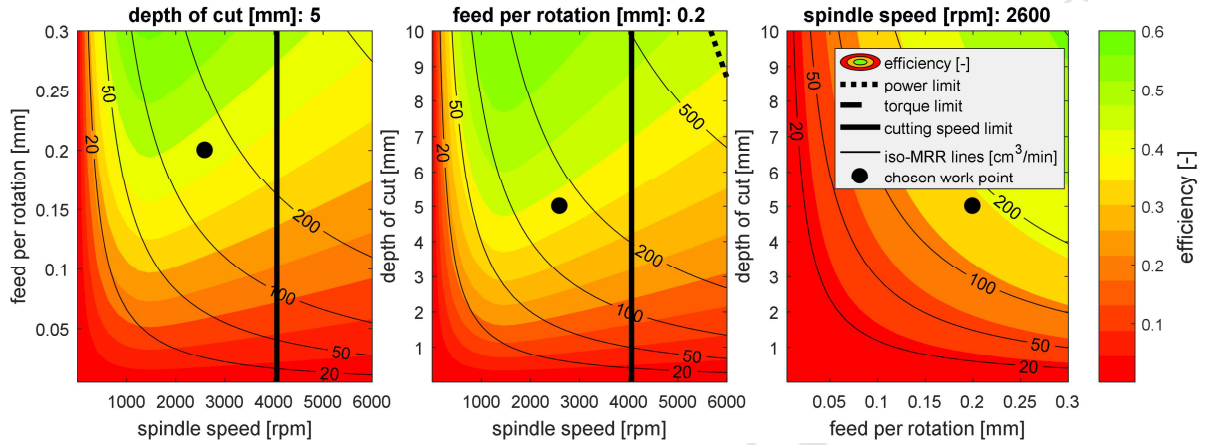| Spindle speed ω [rad/s]	1	6000
Cutting speed v_c [m/min]	-	255
Feed rate f [mm/rev]	0.005	0.3
Depth of cut a_p [mm]	0.1	10
Spindle torque τ_{load} [Nm]	-	350
Spindle power P_{el} [kW]	-	40

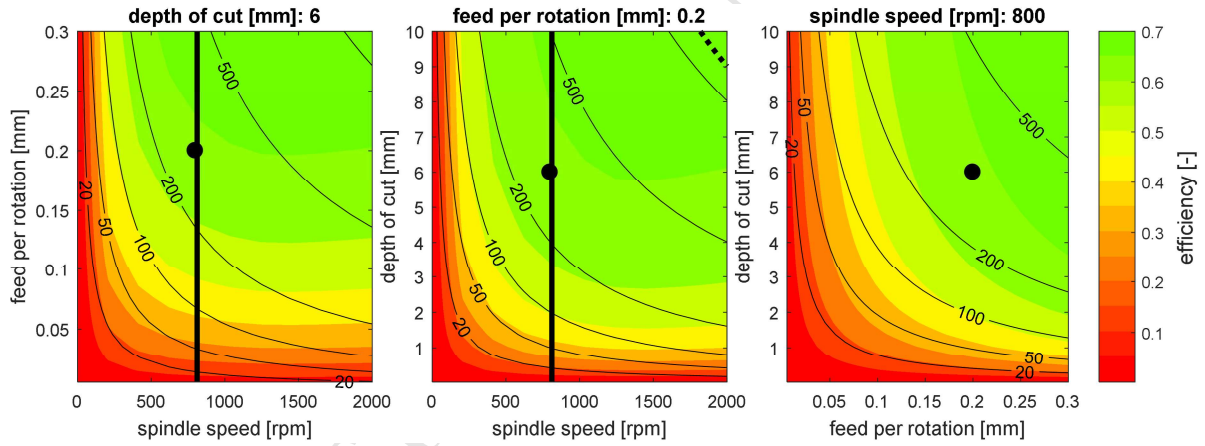Fig. 8. Overall PU efficiency for working diameter of 20mm.

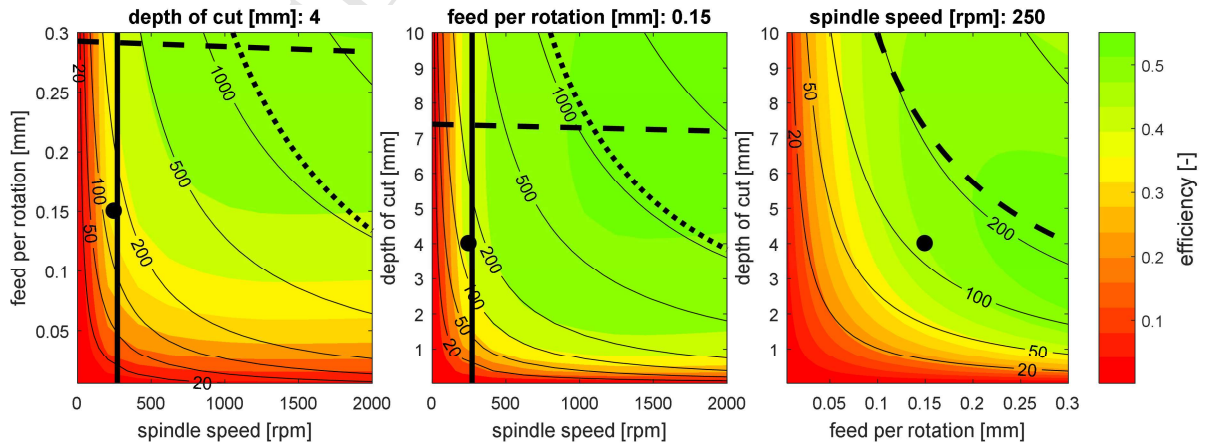Fig. 9. Overall PU efficiency for working diameter of 100mm.

Fig. 10. Overall PU efficiency for working diameter of 300mm.

The efficiency surfaces related to low and medium diameter cutting (Fig. 8 and Fig. 9) reveal that an increase of depth of cut and feed result in a general improvement of process efficiency: both these parameters cause a proportional increment in spindle torque, which produces a strong positive effect on PU efficiency for a wide range of spindle speed (see Fig. 7). In high diameter region (Fig. 10) maximizing a_p and f has limited impact on efficiency, as for its highest values efficiency stays constant or even decreases by few percent. Similar behavior was spotted in experimental study of (Draganescu et al., 2003) in Fig. 3, where for face milling operation was performed using a tool with high diameter (250mm). Achieving highest values of both feed and depth of cut at the same time is not possible because of spindle torque limit, and overall it is better to maximize feed rather than depth of cut, as it this way impact of edge component losses can be reduced (see Eq. (15)).

Whereas for diameters of 100mm and 300mm increasing *MRR* by maximizing cutting parameters increases efficiency, for low diameter turning the effect is no longer that simple: Fig. 8 shows that there is an optimal cutting speed above which efficiency starts to drop. This can be attributed to rapid growth of friction losses and resistive losses (field control related) with speed. Similar phenomenon can be observed in experimental study (Draganescu et al., 2003).

5.3. Optimal cutting parameters in function of *MRR*

Efficiency optimization was performed by searching for cutting parameters which maximize overall efficiency from Eq. (2) but do not violate spindle and tool limits (Eq. (20) and Eq. (21)), for a range of predefined diameters and material removal rates (Table 9). Authors propose to consider two strategies to apply, in an industrial context, the proposed efficiency formulation: with and without considering the basal power component.

Table 9. Optimization ranges

Parameter	Lower limit	Upper limit	No. of values
workpiece diameter (d') [mm]	5	200	80
material removal rate (MRR') [mm^3/min]	$0.1 MRR_{max}(d)$	$MRR_{max}(d)$	25

Strategy one (Fig. 11): Completion time on the cutting operation determines turn-on time of the machine. In this case, basal power of the PU and the whole machine affects the energy performance of the material removal process as discussed in section 2.6. This is a typical case for a standalone machine with a single spindle, where the machine is turned off, or put into energy saving mode while not in use.

Strategy two (Fig. 12): Machine is always on during shift but is not fully utilized (e.g. often waiting for part arrival from upstream machines). Is such a scenario the machine consumes the same amount of basal power independently on the actual *MRR*. Similarly, in a multi-spindle machine with cycle unbalance between the various spindles, the non-bottlenecking spindles may not work at highest *MRR* if it produces energy saving. In this scenario, machine basal consumption P_0 and chillers basal power P_b are not considered, been a constant factor during optimization.
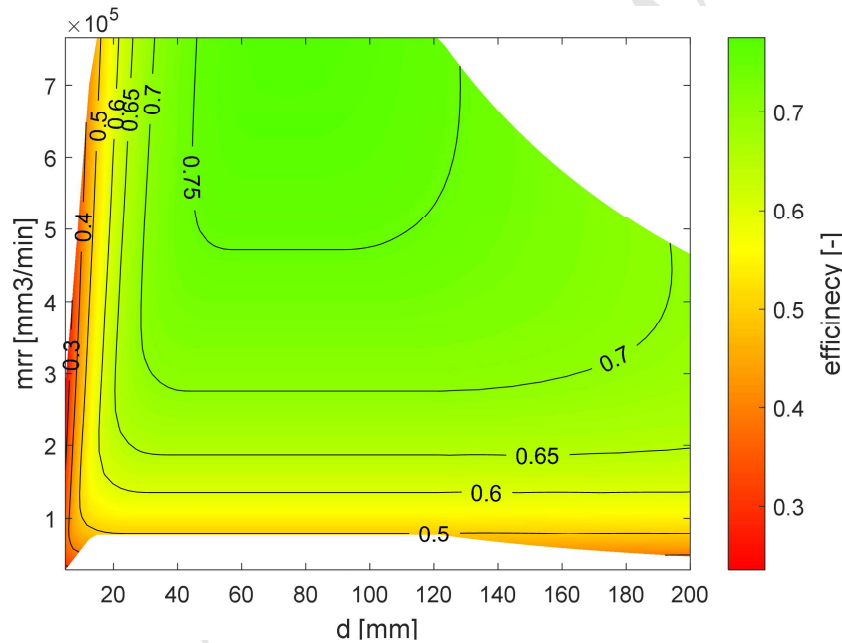

Fig. 11. Maximized PU efficiency of material removal for a given forced MRR and cutting diameter d including chiller basal power term (*Strategy 1*)
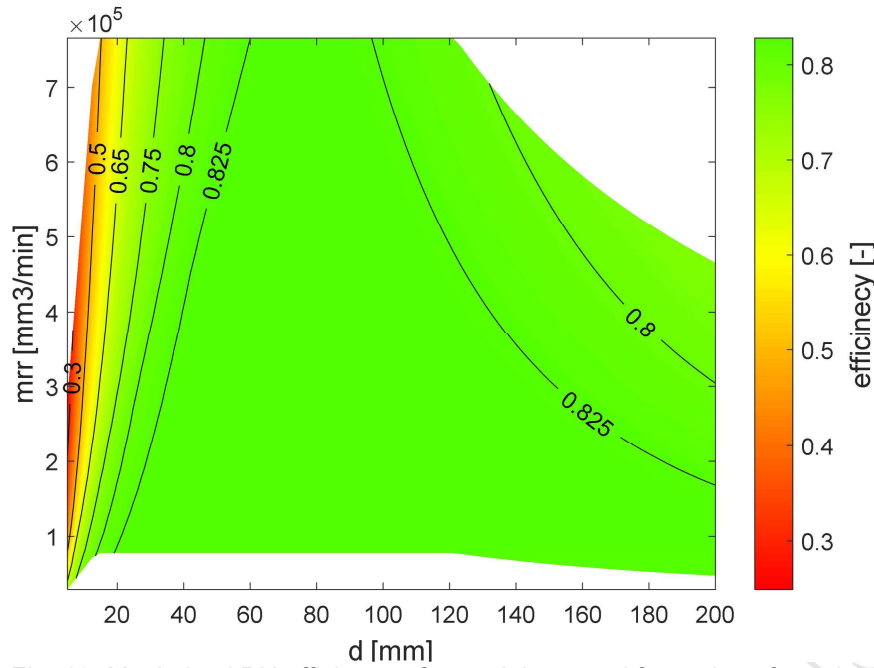
Fig. 12. Maximized PU efficiency of material removal for a given forced MRR and cutting diameter d. excluding chiller basal power term (*Strategy 2*).

For clarity, each strategy will be discussed separately, distinguishing three workpiece diameter regions: small (up to 40mm), medium (40-120mm) and large diameter (more than 120mm).

Scenario one – small diameter: efficiency is lowest in this region (25-60%), and is decreasing with decreasing diameter. Maximum productivity is also low, limited by spindles top speed (6500rpm). Highest efficiency for a given diameter is not achieved for maximum MRR value but there is a visible optimum. For smallest considered diameter (5mm), reducing MRR from highest $28.4 \cdot 10^4$ mm^3/min to optimal $8.1 \cdot 10^4$ mm^3/min results in efficiency improvement (from 23.5% to 35.9%). Efficiency loss is dominated by friction.

Scenario one – medium diameter: this region is of highest efficiency and productivity, which reach 78% and $76.5 \cdot 10^4$ mm^3/min, respectively. Productivity is limited only by material cutting speed limit. Reducing MRR progressively reduces efficiency.

Scenario one – large diameter: maximum productivity is limited due to maximum spindle torque. Efficiency deteriorates with increasing diameter, from 75% at 120mm to 46% at 200mm. Similar to medium diameter region, decreasing MRR deteriorates efficiency. Main contribution of losses are copper losses, due to high quadrature current component.

Scenario two – small diameter: similar to *Scenario one;* efficiency is low with respect to other regions, but it increases progressively with reduction of *MRR*. For 5mm diameter, efficiency boost from 24.8% to 69.8% is possible solely due to less aggressive material removal strategy. High friction losses, due to high speed operation.

Scenario two – medium diameter: highest efficiency region. Without basal power component, efficiency remains invariant to changing *MRR*, settling at the level of around 83%.

Scenario two – large diameter: efficiency drops slightly with increasing diameter but less intensively with respect to *Scenario one* (from 83% to 76.7%). Slight improvement of up to 6.5% can be achieved by reducing *MRR*. Less intensive production requires less torque, therefore copper losses can be reduced at smaller *MRR*.
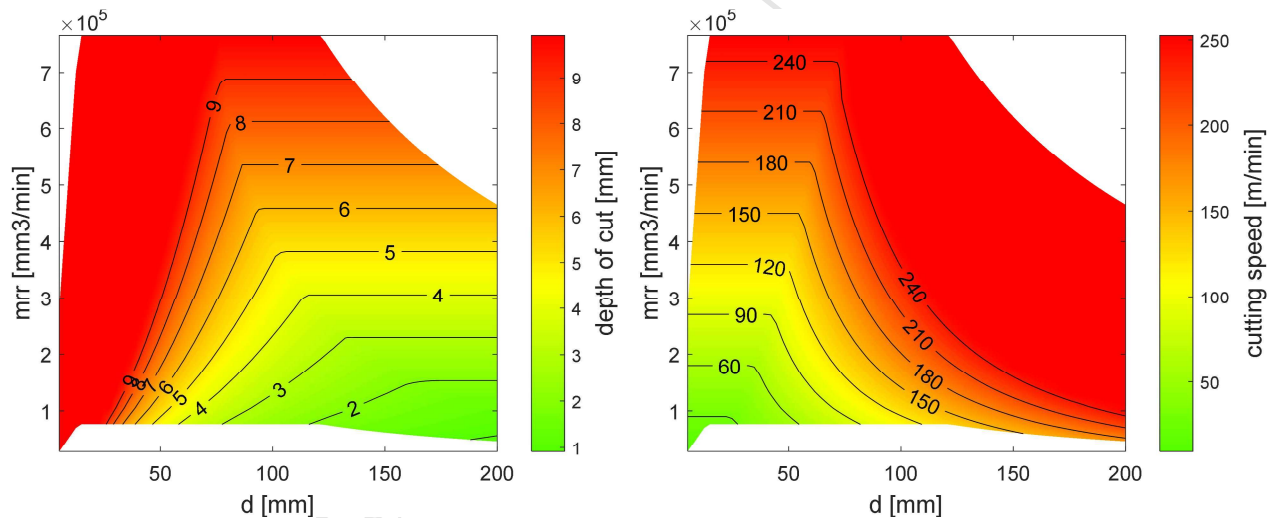

Fig. 13. Cutting parameters maximizing efficiency of material removal process by the considered PU: depth of cut and cutting speed. Feed plot is not shown, as its value assumes always maximum reachable value of 0.35mm/rev.

As far as basal power consumption is neutral from the point of view of minimization (as the basal energy required to remove a given amount of material is fixed, if the *MRR* is given), both scenarios share the same optimal cutting parameter sets, Fig. 13. The third parameter: feed per turn, is always at its maximum value (0.35mm/rev), therefore it has not been plotted: for any diameter and production rate, maximizing feed results in efficiency improvement. Depth of cut and cutting speed are however less trivial. For low diameter range, efficiency can be maximized ensuring highest depth of cut, whereas for large

diameter workpieces it is suggested to maximize cutting speed instead. Mid-range workpieces can be manufactured with a certain optimal combination of both parameters. Appendix B contains spindle, chiller and cutting losses breakdown as well as spindle operating conditions for considered ranges of processing rate and workpiece diameter.

The overall optimization strategy is synthetized in Fig. 14 for different workpiece diameters and productivity (i.e. MRR).The reachable region is limited by both process and machine specification: at low diameters by the maximum spindle speed and tool depth of cut, at high diameters by the maximum spindle torque and tool cutting speed, at high MRR, by the maximum tool feed per turn, cutting speed and depth of cut. The power limit, for the considered spindle, is never reached in the adopted optimization. From Eq.(12), a given MRR can be realized by ∞^2 combinations of parameters $a_p f v_c$. The developed optimization shows that energy per part is minimized always adopting the maximum feed per turn. Additionally, for smaller diameters, the cutting depth should be maximized, while, at higher diameters, the maximum cutting speed should be adopted.
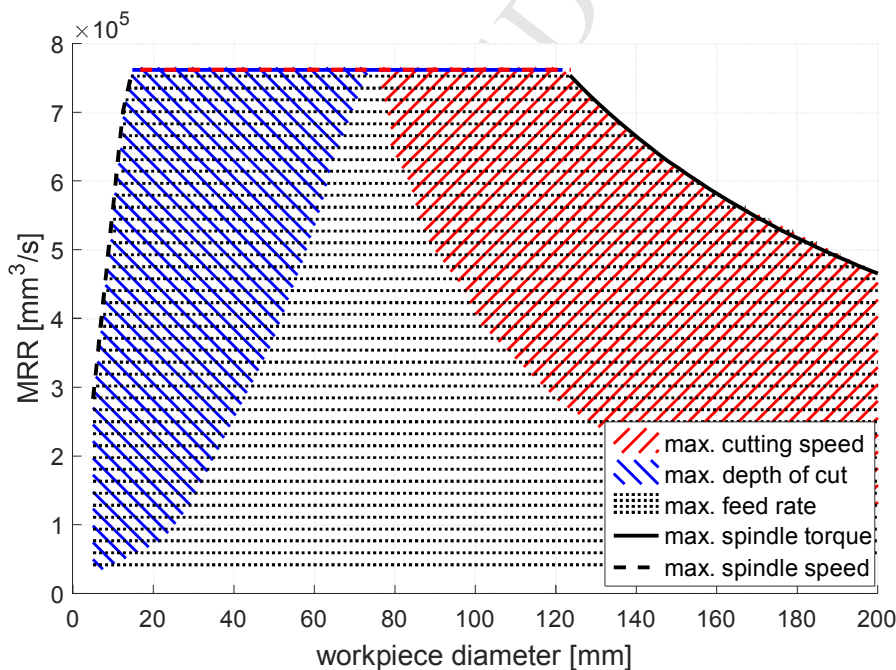

Fig. 14. Constrains that are active in efficiency maximization as function of MRR and workpiece diameter. The highest possible feed must be always selected. Additionally, in the low diameter region, maximization of depth of cut brings the highest efficiency, whereas, for large diameters, highest cutting speed is the optimal choice. Maximum productivity (i.e. maximum MRR) is limited by spindle

speed (for low diameters), by both cutting speed and depth of cut (for intermediate diameters) and by spindle torque (for high diameters).

6. **Discussion**

6.1. Spindle testing method

Proposed method for spindle testing, modelling and identification allows to obtain energy model of PM spindle and estimate its efficiency for the whole operating region. It does not require using external loading motor and a torque sensor because continuous run-up and run-down cycles allow sufficient loading due to inertial forces. Spindle speed and motor currents are measured via machine NC. However, this method requires a fast sampling power meter to compute power at least 50 times per second, for accurate model fitting. Many commercial industrial power meters do not have these qualities. Comparing to experimental efficiency computation with a loading motor, model based energy assessment allows distinguishing between various losses sources, such as friction, copper losses or even cutting losses. It gives additional insights into PU internal, non-measurable quantities and helps to understand which design actions could be undertaken to most effectively improve efficiency in a new generation of machines. Additionally, models support what-if analyses on different manufacturing strategies, as it was performed by the authors in sections 5.1 and 5.2.

6.2. Overall efficiency in cutting process

When combining PU and cutting process efficiencies, the proposed methodology can provide counter-intuitive suggestions for energy optimization of the turning process. It has been pointed out that, in some cases, a *MRR* increase impairs the overall process efficiency. In general, the overall process efficiency is dominated by PU efficiency, therefore, when *MRR* is increased by increasing spindle speed, the overall process efficiency decreases, according to PU efficiency behavior. Nevertheless, cutting efficiency plays a significant role when spindle speeds are low (for example when turning on large diameters, or hard-to-cut materials like titanium alloys). In this case, an increase in the depth of cut causes an

increase in the edge components of cutting force, producing an impairment of efficiency that is not compensated by the slight PU efficiency improvement implied by the torque increase.

6.3. Optimal cutting conditions in function of *MRR* and *d*

Efficiency maps from section 5.3 clearly indicate that efficiency of PU cannot be treated simply as a fixed value and strongly depends on several factors. One driving factor is workpiece size, which was modelled trough parameter *d.* Optimal cutting parameters change significantly as *d* varies, with exception of feed rate which, when maximized, always leads to efficiency improvements. For depth of cut and spindle speed the choice is less trivial, however the general rule could be increasing depth of cut for small diameter ranges and increasing cutting speed for large diameters.

Another dimension to be considered in efficiency analysis of cutting process is *MRR*. Here also choice is not evident and depends also on machine working condition. In *scenario 1,* overall consumption strongly depends on basal power of both chiller and remaining machine peripherals. Potential energy saving trough reduction of *MRR* was only possible for small diameter workpieces, but chosen strategy must be individually weighed against basal consumption of the whole machine. As an obvious consequence, for machines with significant basal consumption, it might be best to always maximize *MRR*. The general tendency in machine tools is to reduce basal consumption through better selection of machine components (chiller, hydraulic units etc.), avoiding oversizing, and using intelligent stand-by modes. Therefore, it's most likely that future generations of machines will exhibit reduced basal consumption and will be able to utilize shown opportunity for energy use reduction via lowering *MRR*.

Scenario 2 showed that, if in a considered production scenario, the basal power consumption is fixed, no matter the activity of the machine, the opportunities to increase processing efficiency arise. Staying at highest productivity in low cutting diameter region indicates high losses due to friction as well as increased resistive losses due to PM motor

field weakening at high speed. Similarly, in the highest diameter region, cutting is performed at the maximum torque, which contributes to i_q-related resistive losses. In both cases, applying a less aggressive processing strategy brings considerable overall energy savings. Charts as the one represented in Fig. 14 are easily computed, for a given turning machine, considering different workpiece materials and tool geometries (i.e. for different sets of cutting parameters), giving useful overall indications to optimize energy efficiency in process planning.

The analysis demonstrated that the efficiency of a spindle subsystem varies significantly with the operating conditions: between low speed heavy operations and high speed light machining the absolute difference in efficiency can reach 50-60%. This fact invalidates, for production scenarios with a wide range of operating parameters, the constant spindle efficiency hypothesis adopted in (Albertelli et al., 2016, Xiong et al., 2016) during cutting parameters optimization.

7. **Conclusions**

A novel integrated approach for energy efficiency optimization in turning operations has been presented, taking into account the strong interrelations between cutting process, spindle with permanent magnet motor and its chiller. The model-based approach, after a reduced set of experiments for model identification, provides general results and additional insight, indicating where and why, in the system, energy dissipations occur.

Tests on a turning machine show the quality of the identified models and provide general guidelines for energy optimization, considering workpieces of different diameters and various production scenarios. On the contrary to the experimental study of (Mori et al., 2011) which showed that efficiency increase can only be achieved by maximization of the processing rate, it has been demonstrated that, in some cases, increasing *MRR* impairs the overall process efficiency. This misalignment can be explained by the fact, that typically experimental studies cover a limited number of operational conditions, whereas the model-

based approach to efficiency analysis, proposed in this article, covers a complete range of operating conditions, including varying workpiece size. As much as 34.5% of saving of the PU energy can be achieved by reducing processing speed in small diameter cutting. Given that the examined permanent magnets spindle + chiller assembly is often used in different machine tool types, the same approach can possibly be extended to similar processes, like drilling and boring. The extension to milling is also achievable, where the d parameter would represent the tool diameter, but it implies the introduction of further parameters concerned with tool engagement and milling path; thus, a consistent energy analysis and optimization would become more complicated.

The provided pre-optimized function, relating efficiency/energy to processing rate (MRR) and workpiece characteristic (namely, diameter d), constitutes a building block which can be used at machine level to support energy use prediction in production optimization. For example, it can be used to optimize process planning for different machine tool configurations, based on the same PU but characterized by diverse peripheral equipment: for each possible processing rate, processing time is easily calculated and then used to compute the corresponding energy consumption of the peripheral units, due to the basal power consumption. The proposed approach will be used, in future developments, to represent the relationship between cycle time and energy use while optimizing a machining cycle on a given machining center.

8. **Acknowledgements**

References

Albertelli, P., Bianchi, G., Bigliani, A., Borgia, S., Matta, A., Zanotti, E., 2011. Evaluation of the energy consumption in machine tools: a combined analytical-experimental approach, in: Proceedings of 13th International Conference on The Modern Information Technology in the Innovation Processes on the Industrial Enterprises. Trondheim, Norway.

Albertelli, P., Keshari, A., Matta, A., 2016. Energy oriented multi cutting parameter optimization in face milling. J. Clean. Prod. 137, 1602–1618. doi:10.1016/j.jclepro.2016.04.012

Altintas, Y., 2012. Manufacturing automation: metal cutting mechanics, machine tool vibrations, and CNC design, 2nd ed. ed. Cambridge University Press, Cambridge ; New York.

Arrazola, P.J., Özel, T., Umbrello, D., Davies, M., Jawahir, I.S., 2013. Recent advances in modelling of metal machining processes. CIRP Ann. - Manuf. Technol. 62, 695–718. doi:10.1016/j.cirp.2013.05.006

Borgia, S., Albertelli, P., Bianchi, G., 2016. A simulation approach for predicting energy use during general milling operations. Int. J. Adv. Manuf. Technol. 1–15. doi:10.1007/s00170-016-9654-5

Borgia, S., Leonesio, M., Bianchi, G., Albertelli, P., 2014a. Machine Tool Energetic Simulation during General Milling Operations, in: Innovations of Sustainable Production for Green Mobility - Energy-Efficient Technologies in Production. Presented at the 3rd International Chemnitz Manufacturing Colloquium ICMC 2014, pp. 583–599.

Borgia, S., Pellegrinelli, S., Bianchi, G., Leonesio, M., 2014b. A Reduced Model for Energy Consumption Analysis in Milling. Procedia CIRP, Variety Management in Manufacturing 17, 529–534. doi:10.1016/j.procir.2014.01.105

Bort, G., Carlos, M., Leonesio, M., Bosetti, P., 2016. A model-based adaptive controller for chatter mitigation and productivity enhancement in CNC milling machines. Robot. Comput.-Integr. Manuf. 40, 34–43. doi:10.1016/j.rcim.2016.01.006

Calvanese, M.L., Albertelli, P., Matta, A., Taisch, M., 2013. Analysis of Energy Consumption in CNC Machining Centers and Determination of Optimal Cutting Conditions, in: Re-Engineering Manufacturing for Sustainability. Springer, Singapore, pp. 227–232. doi:10.1007/978-981-4451-48-2_37

Diaz, N., Helu, M., Dornfeld, D., 2010. Design and Operation Strategies for Green Machine Tool Development. Lab. Manuf. Sustain.

Diaz, N., Redelsheimer, E., Dornfeld, D., 2011. Energy Consumption Characterization and Reduction Strategies for Milling Machine Tool Use, in: Glocalized Solutions for Sustainability in Manufacturing. Springer, Berlin, Heidelberg, pp. 263–267. doi:10.1007/978-3-642-19692-8_46

Dong, Y.H., Xu, H.T., Lin, H., 2009. Simulation of Cutting Force in Turning Machining Process on CK7815 NC Lathe. Key Eng. Mater. 392–394, 64–68. doi:10.4028/www.scientific.net/KEM.392-394.64

Draganescu, F., Gheorghe, M., Doicin, C.V., 2003. Models of machine tool efficiency and specific consumed energy. J. Mater. Process. Technol. 141, 9–15. doi:10.1016/S0924-0136(02)00930-5

Drury, B., 2001. Control Techniques Drives and Controls Handbook. IET.

Duflou, J.R., Sutherland, J.W., Dornfeld, D., Herrmann, C., Jeswiet, J., Kara, S., Hauschild, M., Kellens, K., 2012. Towards Energy and Resource Efficient Manufacturing: A Processes and Systems Approach. CIRP Ann. - Manuf. Technol. 61.

Ehmann, K.F., Kapoor, S.G., DeVor, R.E., Lazoglu, I., 1997. Machining Process Modeling: A Review. J. Manuf. Sci. Eng. 119, 655. doi:10.1115/1.2836805

Geletu, A., 2007. Solving optimization problems using the matlab optimization toolbox-a tutorial. TU-Ilmenau, Fakultät für Mathematik und Naturwissenschaften.

Hazewinkel, M. (Ed.), 1988. Encyclopaedia of mathematics: an updated and annotated translation of the Soviet "Mathematical encyclopaedia." Reidel ; Sold and distributed in the U.S.A. and Canada by Kluwer Academic Publishers, Dordrecht ; Boston : Norwell, MA, U.S.A.

Leonesio, M., Tosatti, L.M., Pellegrinelli, S., Valente, A., 2012. An Integrated Approach for Joint Process Planning and Machine Tool Dynamic Behavioral Assessment. Procedia CIRP, 1st CIRP Global Web Conference: Interdisciplinary Research in Production Engineering (CIRPE2012) 2, 38–43. doi:10.1016/j.procir.2012.05.036

Marquardt, D., 1963. An Algorithm for Least-Squares Estimation of Nonlinear Parameters. J. Soc. Ind. Appl. Math. 11, 431–441. doi:10.1137/0111030

Mori, M., Fujishima, M., Inamasu, Y., Oda, Y., 2011. A study on energy efficiency improvement for machine tools. CIRP Ann. - Manuf. Technol. 60, 145–148. doi:10.1016/j.cirp.2011.03.099

Peng, T.V., Xu, X., 2013. A Universal Hybrid Energy Consumption Model for CNC Machining Systems, in: Nee, A.Y.C., Song, B., Ong, S.-K. (Eds.), Re-Engineering Manufacturing for Sustainability. Springer Singapore, pp. 251–256.

Stone, M., 1974. Cross-Validatory Choice and Assessment of Statistical Predictions. J. R. Stat. Soc. Ser. B Methodol. 36, 111–147. doi:10.2307/2984809

Wójcicki, J., Borgia, S., Bianchi, G., 2016. Fast Experimental Energy Characterization of a Controlled Rotary Axis. Procedia CIRP, Research and Innovation in Manufacturing: Key Enabling Technologies for the Factories of the Future - Proceedings of the 48th CIRP Conference on Manufacturing Systems 41, 323–328. doi:10.1016/j.procir.2015.10.003

Xiong, Y., Wu, J., Deng, C., Wang, Y., 2016. Machining process parameters optimization for heavy-duty CNC machine tools in sustainable manufacturing. Int. J. Adv. Manuf. Technol. 87, 1237–1246. doi:10.1007/s00170-013-4881-5

Yang, W.H., Tarng, Y.S., 1998. Design optimization of cutting parameters for turning operations based on the Taguchi method. J. Mater. Process. Technol. 84, 122–129. doi:10.1016/S0924-0136(98)00079-X

Zhou, L., Li, Jianfeng, Li, F., Meng, Q., Li, Jing, Xu, X., 2016. Energy consumption model and energy efficiency of machine tools: a comprehensive literature review. J. Clean. Prod. 112, Part 5, 3721–3734. doi:10.1016/j.jclepro.2015.05.093

Appendix A – Nomenclature

Parameter name	Symbol
average cut diameter [mm]	d
basal energy consumption [J]	E_0
chiller basal consumption [W]	P_b
chiller heat load function [W]	P_h
chiller effectiveness coefficient [-]	θ
chiller unit electrical power demand [W]	$P_{chiller}$
cutting coefficient associated to the edge component of tangential cutting force [N/mm]	k_{te}
cutting coefficient associated to material shear [N/mm^2]	k_{tc}
cutting torque [Nm]	τ_{cutt}
cutting power [W]	P_c
cutting speed [m/min]	v_c
depth of cut [mm]	a_p
direct current component [A]	i_d
efficiency of cutting process [-]	η_{cut}
efficiency of spindle and chiller assembly [-]	η_{PU}
efficiency (maximized through optimization) [-]	η_{max}
efficiency (overall) [-]	η
feed rate (per turn) [mm]	f
field weakening coefficient [A·rad/s]	α
field weakening coefficient [-]	β

field weakening starting speed [rad/s]	ω_0
machine basal power loss [W]	P_0
material removal rate [mm³/min]	MRR
material removal mechanical energy [J]	E_{mech}
mechanical specific energy $k_c = \frac{P_c}{MRR}$ [N/mm²]	k_c
overall specific energy [N/mm²]	e_c
processing unit energy consumption [J]	E_{PU}
quadrature current component [A]	i_q
resistive losses in the motor [W]	$P_{mot\,loss}$
spindle motor load torque [Nm]	τ_{load}
spindle external load torque (process and inertia)	τ
spindle motor electrical power demand [W]	P_{el}
spindle speed [rad/s]	ω
spindle speed limit [rad/s]	ω_{max}
spindle power limit [W]	P_{max}
spindle torque limit [Nm]	τ_{max}
static friction coefficient [Nm]	μ_s
tangential component of the cutting force [N]	F_c
torque constant [Nm/A]	K_T
total spindle moment of inertia [kg·m²]	J
total energy consumption [J]	E_c
viscous friction coefficient [Nm·s/rad]	μ_v
winding resistance [Ω]	R

Appendix B – Spindle operating condition and losses breakdown

Spindle load torque and speed while operating in an optimal cutting condition are presented in Fig. 15. Energy losses for *Scenario one* (subsection 5.3) as a fraction of total energy demand were computed and classified by cause: friction losses (spindle bearings and process edge component) in Fig. 16, motor resistive losses with separated quadrature and direct current parts in Fig. 17 and chiller consumption in Fig. 18.
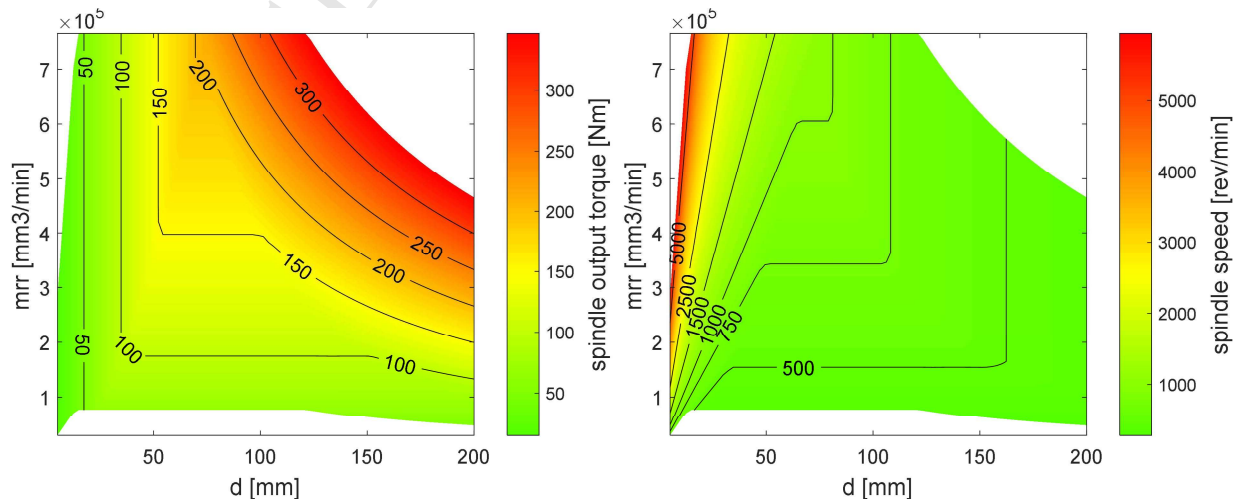
Fig. 15. Spindle operation in highest efficiency condition: a) spindle speed; b) spindle torque
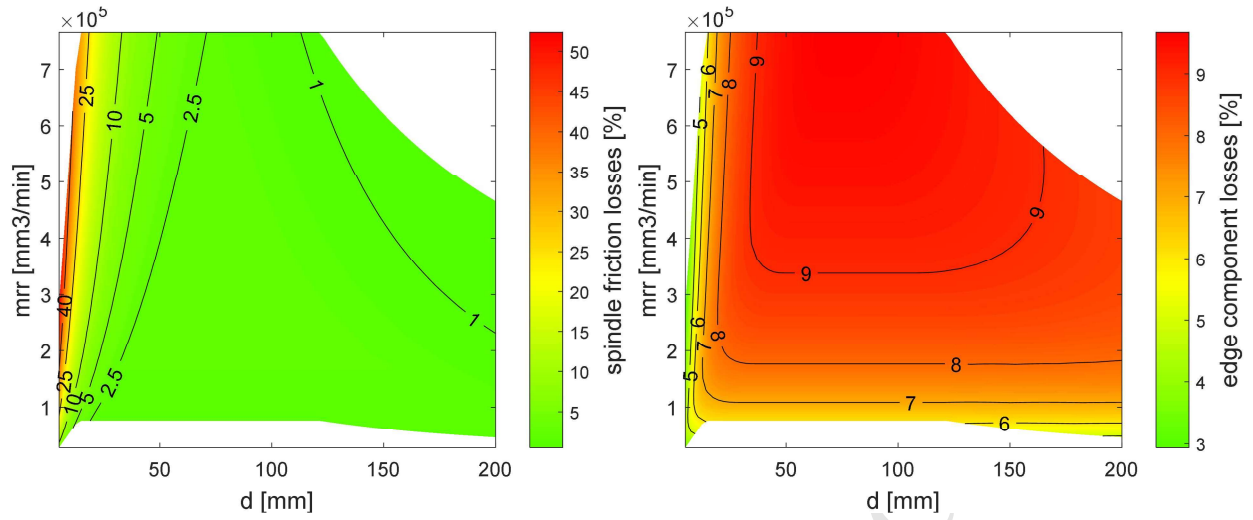

Fig. 16. Share of friction losses in overall energy use in highest efficiency condition: a) spindle friction losses; b) cutting losses due to edge component
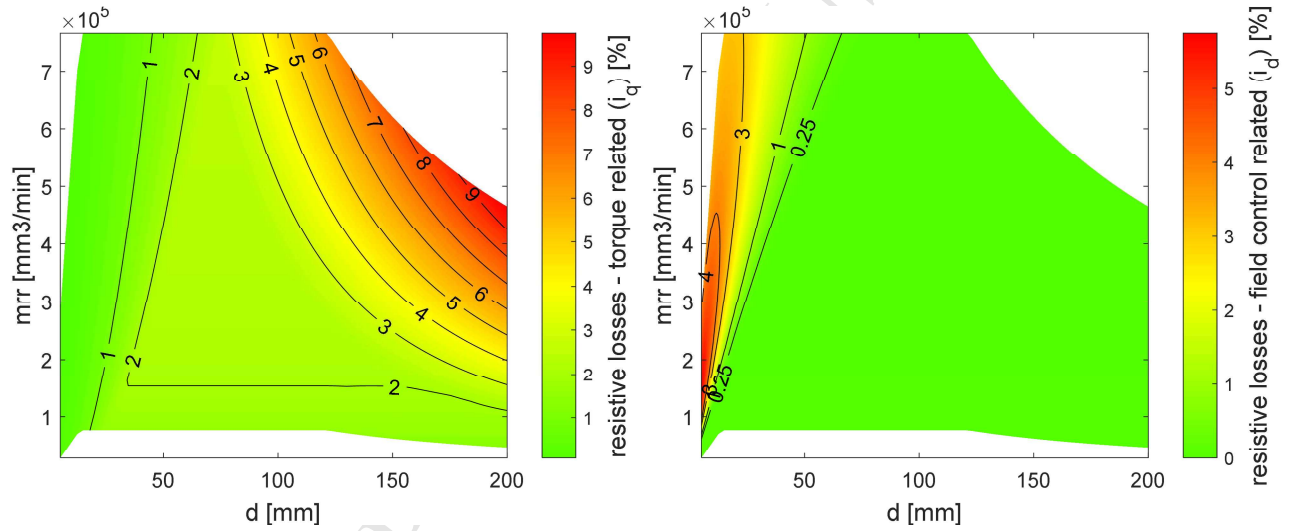

Fig. 17. Share of resistive losses of spindle motor in overall energy use in highest efficiency condition: a) due to torque generation related; b) due to motor field weakening
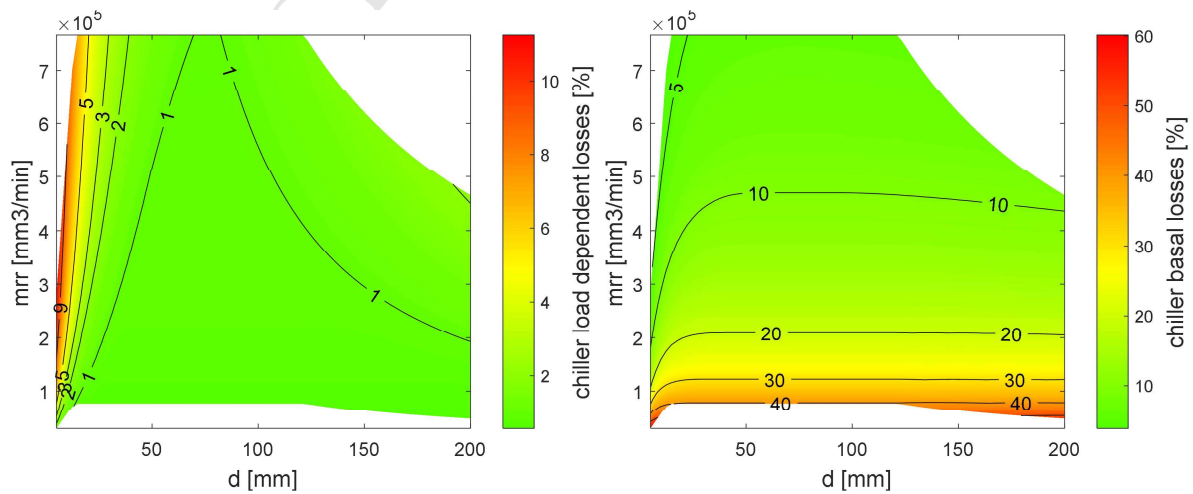
Fig. 18. Share of chiller consumption (losses) in overall energy use in highest efficiency conditions a) load dependent (varying) consumption; b) basal consumption

Highlights

- Model-based energy assessment for spindle-chiller assembly is proposed
- Efficiency model is a function of workpiece diameter and material removal rate
- Reduction of material removal rate can bring energy savings in low diameter cutting
- Procedure can be automated using machine tool control and, therefore, widely adopted